Inversion of P-wave data in laterally heterogeneous VTI media. Part I: Plane dipping interfaces

Vladimir Grechka, Andrés Pech and Ilya Tsvankin
Center for Wave Phenomena, Department of Geophysics, Colorado School of Mines, Golden, CO 80401-1887

ABSTRACT

A major complication caused by anisotropy in velocity analysis and imaging is the uncertainty in estimating the vertical velocity and depth scale of the model from surface data. For transversely isotropic models with a vertical symmetry axis (VTI media), P-wave kinematic signatures are governed by the vertical velocity V_{P0} and Thomsen anisotropic parameters ϵ and δ. However, only two combinations of these parameters – the NMO velocity from a horizontal reflector $V_{\rm nmo}(0)$ and the anellipticity coefficient η – can be determined from P-wave reflection traveltimes, if the medium above the reflector is laterally homogeneous. As a result, P-wave surface data have to be combined with other information (e.g., borehole data or converted waves) to build velocity models for depth imaging.

The presence of lateral heterogeneity in the overburden may create the dependence of P-wave reflection data on all three relevant parameters (V_{P0}, ϵ and δ) and, therefore, may help to determine the depth scale of the velocity field. Here, we examine parameter estimation in VTI media composed of homogeneous layers separated by plane dipping interfaces. In general, for non-intersecting interfaces the interval parameters cannot be recovered from P-wave moveout in a unique way.

Nonetheless, if the reflectors have sufficiently different azimuths, *a priori* knowledge of any *single* interval parameter makes it possible to reconstruct the whole model in depth. For example, the parameter estimation becomes unique if the subsurface layer is known to be isotropic. In the case of 2-D inversion on the dip line of co-oriented reflectors, it is necessary to specify one parameter per layer (e.g., in VSP surveys it is possible to determine the vertical velocity). Furthermore, no *a priori* information is needed for some types of VTI models with irregular interfaces or faults.

Key words: P-waves, VTI media, dipping intermediate interfaces

Introduction

Vertical transverse isotropy, which is believed to be the most common anisotropic model for sedimentary basins, may have a significant impact on velocity analysis and imaging of reflection data. It is well known that the kinematics of P-waves in VTI media is controlled by the vertical velocity V_{P0} and Thomsen's (1986) anisotropic coefficients ϵ and δ (Tsvankin, 1996). Estimation of these parameters from reflection data is a major problem in building accurate velocity models for seismic imaging.

Inversion of P-wave data in VTI media was addressed in a number of recent publications, including Bube and Meadows (1997), Grechka and Tsvankin (1998), Bartel et al. (1998), Le Stunff and Grenié (1998), Le Stunff and Jeannot (1998) and Sexton and Williamson (1998). *Time-domain* imaging for vertical transverse isotropy is largely based on the result of Alkhalifah and Tsvankin (1995) who proved that P-wave reflection traveltimes in laterally homogeneous VTI media above a dipping interface depend on just two pa-

rameters – the normal-moveout (NMO) velocity from a horizontal (zero-dip) reflector,

$$V_{\rm nmo}(0) = V_{P0}\sqrt{1+2\,\delta}\,, \tag{1}$$

and the anellipticity coefficient denoted as η,

$$\eta \equiv \frac{\epsilon-\delta}{1+2\,\delta}\,. \tag{2}$$

Although $V_{\rm nmo}(0)$ and η provide enough information for time processing, they are not sufficient for resolving the vertical velocity V_{P0} and reflector depth. Therefore, surface P-wave data do not constrain the depth scale in VTI media needed, for example, in prestack depth migration.

The two-parameter description of P-wave time-domain signatures, however, breaks down in the presence of lateral heterogeneity above the reflector (Alkhalifah et al., 1998; Grechka and Tsvankin, 1999b). Grechka and Tsvankin (1999b) developed a Dix-type averaging procedure for NMO velocities in laterally heterogeneous anisotropic media and applied it to moveout analysis for vertical transverse isotropy. Their results show that the NMO velocity of reflected P–arrivals which cross dipping intermediate interfaces depends on the individual values of V_{P0}, ϵ, and δ, rather than on the combinations $V_{\rm nmo}(0)$ and η. Le Stunff et al. (1999) presented an example of successful inversion of P-wave traveltimes for the parameters V_{P0}, ϵ and δ in a model that included a dipping VTI layer overlying a purely isotropic medium.

Here, we discuss P-wave moveout inversion for more complicated VTI models composed of multiple homogeneous layers separated by plane dipping interfaces. Our analysis shows that 3-D wide-azimuth P-wave moveout data from N model non-intersecting interfaces constrain up to $3N-1$ combinations of the interval parameters $V_{P0,n}$, ϵ_n, δ_n, where $n=1,\ldots,N$. Hence, to determine the interval values $V_{P0,n}$, ϵ_n, and δ_n uniquely and reconstruct the model in depth, at least one of the parameters has to be known *a priori*. The inversion is generally better posed if the subsurface contains faults or the interfaces are curved (but the layers are still homogeneous). A more detailed discussion of P-wave traveltime inversion for VTI media with irregular interfaces is given in a sequel paper (Part II).

Analytic background

VTI model and data for inversion

We consider a model composed of N homogeneous VTI layers (some of them may be isotropic) separated by plane dipping non-intersecting interfaces (Figure 1). The model parameters responsible for P-wave kinematics include the interval vertical velocities $V_{P0,n}$, anisotropic coefficients ϵ_n and δ_n, and the interface dips ϕ_n, azimuths ψ_n and depths z_n (the depth can be measured,

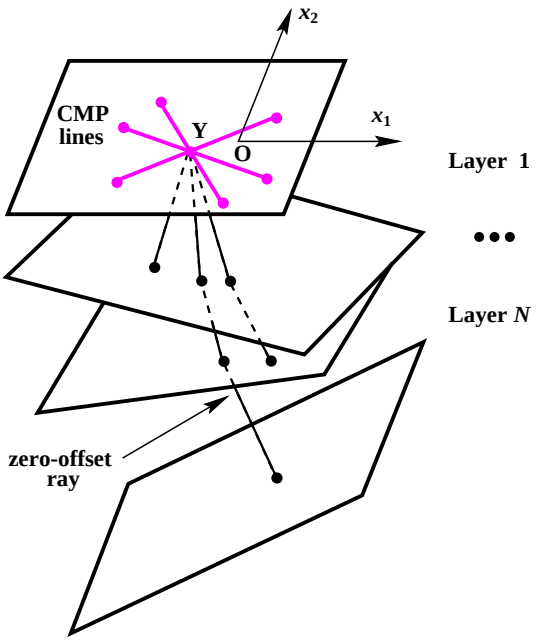

Figure 1. Azimuthally-dependent reflection traveltimes are recorded over a stack of VTI layers separated by plane dipping interfaces.

for example, under the coordinate origin **O**). Thus, the model vector

$$\mathbf{m} \equiv \{V_{P0,n},\, \epsilon_n,\, \delta_n,\, \phi_n,\, \psi_n,\, z_n\}\,, \quad (n=1,\,\ldots,\,N) \tag{3}$$

is characterized by $6N$ independent quantities. It is convenient to split the vector $\mathbf{m}$ into two vectors $\mathbf{l}$ and $\mathbf{i}$, where $\mathbf{l}$ contains the layer parameters,

$$\mathbf{l} \equiv \{V_{P0,n},\, \epsilon_n,\, \delta_n\}\,, \quad (n=1,\,\ldots,\,N)\,, \tag{4}$$

and $\mathbf{i}$ describes the interfaces,

$$\mathbf{i} \equiv \{\phi_n,\, \psi_n,\, z_n\}\,, \quad (n=1,\,\ldots,\,N)\,. \tag{5}$$

Clearly, each vector ($\mathbf{l}$ and $\mathbf{i}$) has $3N$ components.

Velocity analysis of 3-D multi-azimuth P-wave data recorded at common midpoints (CMP) with the coordinates $\mathbf{Y}=[Y_1,\,Y_2]$ can provide the one-way zero-offset reflection traveltimes $\tau_0(\mathbf{Y},\,n)$ from all interfaces and the corresponding NMO velocities $V_{\rm nmo}(\alpha)$ (α is the azimuth). Azimuthally dependent NMO velocity of any pure mode is described by an ellipse that can be expressed in terms of a 2×2 symmetric matrix $\mathbf{W}$ (Grechka and Tsvankin, 1998):

$$V_{\rm nmo}^{-2}(\alpha) = W_{11}\cos^2\alpha + 2\,W_{12}\sin\alpha\cos\alpha + W_{22}\sin^2\alpha\,, \tag{6}$$

where

$$W_{ij} = \tau_0\,\frac{\partial^2\tau}{\partial x_i\partial x_j}\bigg|_{\mathbf{Y}} = \tau_0\,\frac{\partial p_i}{\partial x_j}\bigg|_{\mathbf{Y}}\,, \qquad (i,j=1,2)\,. \tag{7}$$

Here $\tau(x_1,\,x_2)$ is the one-way traveltime from the zero-

offset reflection point to the location $\mathbf{x}\{x_1, x_2\}$ at the surface, τ_0 is the one-way zero-offset traveltime, and p_i are the components of the slowness vector corresponding to the ray recorded at the point $\mathbf{x}$.

The matrices $\mathbf{W}(\mathbf{Y}, n)$ can be obtained from azimuthal velocity analysis based on the hyperbolic moveout equation parameterized by the NMO ellipse, as described by Grechka and Tsvankin (1999a). Using the zero-offset (or stacked) time sections of reflection events, we can pick the reflection slopes and determine the ray parameters $\mathbf{p}(\mathbf{Y}, n) = [p_1(\mathbf{Y}, n), p_2(\mathbf{Y}, n)]$ of the zero-offset rays.

Since the layers in our model are homogeneous and the interfaces are plane (Figure 1), the slowness components $p_1(\mathbf{Y}, n)$, $p_2(\mathbf{Y}, n)$ are independent of the CMP coordinate $\mathbf{Y}$. Taking into account that

$$\frac{\partial \tau_0(\mathbf{Y}, n)}{\partial Y_j} = p_j(n)\,, \quad (j = 1, 2)\,, \tag{8}$$

the traveltimes $\tau_0(\mathbf{Y}, n)$ can be expressed as *linear* functions of Y_j:

$$\tau_0(\mathbf{Y}, n) = \tau_0(\mathbf{O}, n) + p_1(n)\, Y_1 + p_2(n)\, Y_2\,. \tag{9}$$

Here $\tau_0(\mathbf{O}, n)$ are the traveltimes recorded at the coordinate origin $\mathbf{O}$. Using equation (9), the input traveltime data $\mathbf{d}(\mathbf{Y}, n)$ can be represented in the following form:

$$\mathbf{d}(\mathbf{Y}, n) \equiv \{\tau_0(\mathbf{O}, n),\, p_1(n),\, p_2(n), \\ W_{11}(\mathbf{Y}, n),\, W_{12}(\mathbf{Y}, n),\, W_{22}(\mathbf{Y}, n)\}\,, \tag{10}$$

where $n = 1, \ldots, N$.

The feasibility of the inversion for $\mathbf{m}$ is controlled by the character of the spatial variation of the effective NMO ellipses $\mathbf{W}(\mathbf{Y}, n)$. To analyze the dependence of $\mathbf{W}$ on the CMP coordinate $\mathbf{Y}$, we next review the procedure of building effective NMO ellipses in laterally heterogeneous media.

Effective NMO ellipse

Grechka and Tsvankin (1999b) introduced the concept of *NMO-velocity surfaces* and used it to develop a methodology for obtaining effective NMO ellipses $\mathbf{W}$ in laterally heterogeneous anisotropic media. Two relevant results of their work applicable to the model at hand can be summarized as follows:

(1) The NMO-velocity surface of any pure reflection mode is obtained by plotting NMO velocity as the radius-vector from a common midpoint along all possible directions of CMP lines in 3-D space. If the medium near the CMP location is locally homogeneous, such a surface is always a cylinder, with the axis pointing in the direction of the zero-offset ray.

(2) The Dix-type averaging procedure of Grechka et al. (1999) is applicable to the *intersections* $\mathbf{W}_n(\mathbf{Y})$ of the interval NMO-velocity cylinders by the model interfaces. Each interval cylinder is computed for a fictitious reflector orthogonal to the slowness vector of the interval zero-offset ray. For example, suppose the model contains two layers separated by a dipping interface (Figure 2). Then the intersection $\bar{\mathbf{W}}(\mathbf{Y}, 2)$ of the effective NMO-velocity cylinder (measured at the surface) with a plane parallel to the intermediate interface is obtained from the following Dix-type averaging formula:

$$\tau_0(\mathbf{Y}, 2)\, \left[\bar{\mathbf{W}}(\mathbf{Y}, 2)\right]^{-1} = \tau_{0,1}(\mathbf{Y})\, [\mathbf{W}_1(\mathbf{Y})]^{-1} \\ + \tau_{0,2}(\mathbf{Y})\, [\mathbf{W}_2(\mathbf{Y})]^{-1}\,, \tag{11}$$

where $\tau_{0,1}$ and $\tau_{0,2}$ are the interval zero-offset traveltimes, $\mathbf{W}_1(\mathbf{Y})$ (shaded in gray) and $\mathbf{W}_2(\mathbf{Y})$ (dashed) are the intersections of the NMO-velocity cylinders in the first and second layer with the intermediate interface. The ellipse described by $\bar{\mathbf{W}}(\mathbf{Y}, 2)$ is then projected along the effective NMO-velocity cylinder onto the horizontal plane to find the effective NMO ellipse $\mathbf{W}(\mathbf{Y}, 2)$.

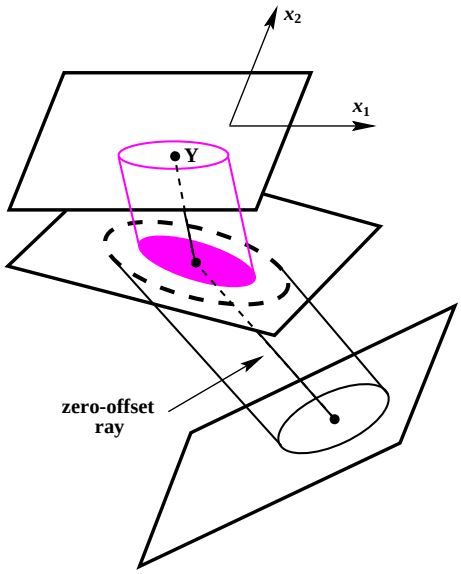

Figure 2. Generalized Dix-type formula (11) averages the intersections of the interval NMO-velocity cylinders with the model interfaces along the zero-offset raypath.

In the model treated here (Figure 1), zero-offset ray trajectories from the same interface are parallel to each other at different CMP locations $\mathbf{Y}$. As a result, the interval slownesses, group-velocity vectors and the matrices $\mathbf{W}_n$ [equation (11)] are independent of the CMP coordinate $\mathbf{Y}$, whereas the interval traveltimes $\tau_{0,n}(\mathbf{Y})$ are *linear* functions of $\mathbf{Y}$. Therefore, the difference between the NMO ellipses $\mathbf{W}(\mathbf{O}, n)$ and $\mathbf{W}(\mathbf{Y}, n)$ measured at points $\mathbf{O}$ and $\mathbf{Y}$ has a purely geometric nature related

to the variations in the length of the interval ray segments. This suggests that the dependence of $\mathbf{W}(\mathbf{Y},\, n)$ on $\mathbf{Y}$ does not provide any information about the model parameters not contained in the NMO ellipses $\mathbf{W}(\mathbf{O},\, n)$. This statement is supported by numerical results below.

Thus, the data vector (10) can be written as

$$\mathbf{d}(\mathbf{Y},\, n) = \{\mathbf{d}(\mathbf{O},\, n),\, \mathbf{Y} - \mathbf{O}\}\,. \tag{12}$$

Feasibility of parameter estimation

It is clear from equation (12) that although traveltime data from different common midpoints may be useful in practice to suppress noise, they give the same information about the medium parameters as the data vector

$$\mathbf{d}(\mathbf{O},\, n) = \{\tau_0(\mathbf{O},\, n),\, \mathbf{p}(n),\, \mathbf{W}(\mathbf{O},\, n)\} \tag{13}$$

at a single CMP. Thus, analyzing the dependence of the vector $\mathbf{d}(\mathbf{O},\, n)$ on the parameter vector $\mathbf{m}$ [equation (3)] should be sufficient for evaluating the feasibility of the inversion. For brevity, henceforth the CMP coordinate will be omitted.

For an N-layered VTI model, the vectors $\mathbf{d}$ and $\mathbf{m}$ contain $6N$ components each. Therefore, the vector $\mathbf{m}$ can be obtained from the data $\mathbf{d}$ only if all components of $\mathbf{d}$ are independent. Unfortunately, this is not the case for VTI media. The P-wave NMO ellipse $\mathbf{W}(1)$ from a dipping reflector overlaid by a homogeneous VTI medium provides only two equations for the medium parameters because its orientation is fixed by the reflector azimuth ψ_1 (Grechka and Tsvankin, 1998):

$$\begin{aligned}\tan\psi_1 &= \frac{p_2(1)}{p_1(1)} \\ &= \frac{1}{2\,W_{12}(1)}\left(W_{22}(1) - W_{11}(1)\right. \\ &\qquad \left. + \sqrt{[W_{22}(1) - W_{11}(1)]^2 + 4\,W_{12}^2(1)}\right)\end{aligned} \tag{14}$$

Specifically, the semi-axes of the NMO ellipse in the first layer constrain the zero-dip NMO velocity $V_{\rm nmo}(0)$ and the anellipticity coefficient η [equations (1) and (2)]. As a result, the data vector in the top layer contains only five components. Singular-value decomposition (SVD) analysis performed below shows that this is the *only* relationship between the components of the data vector, if all interfaces have different strikes.

For inversion purposes, it is convenient to split the vector $\mathbf{d}(\mathbf{O},\, n)$ into two parts. For a given ("trial") set of the interval VTI parameters $\mathbf{l}_n$ [equation (4)], the values of $\tau_0(n)$ and the horizontal slownesses $p_1(n)$, $p_2(n)$ can be used to determine the depths, dips and azimuths of the interfaces $\mathbf{i}_n$ [equation (5)]. Indeed, knowledge of the parameters of the first layer $\tilde{\mathbf{l}}_1$ is sufficient for computing the vertical slowness component from the Christoffel equation and obtaining the slowness vector $\mathbf{p}(1)$. Since the slowness vector of the zero-offset ray is orthogonal to the reflector, the vector $\mathbf{p}(1)$ defines the reflector normal. Then we can find the group-velocity vector (ray) in the first layer and use the traveltime $\tau_0(1)$ to determine the depth z_1 of the first reflector.

Once the first interface has been reconstructed, the slowness vector in the second layer can be obtained from Snell's law and used to find the orientation of the second reflector. The zero-offset traveltime of the reflection from the second interface gives an estimate of the reflector depth, etc. Continuing this procedure downward yields the dips, strikes (or azimuths) and depths of all interfaces of the trial model. Evidently, any errors in the input data or trial layer parameters $\tilde{\mathbf{l}}_n$ will distort the interfaces $\tilde{\mathbf{i}}_n$.

Then the best-fit vector of the layer parameters $\mathbf{l}_n$ has to be found by inverting the NMO ellipses $\mathbf{W}(n)$ because the rest of the input data was used to determine the interfaces. Therefore, to study the feasibility of the inversion procedure it is sufficient to perform SVD analysis of the $3N \times 3N$ matrix of Frechét derivatives

$$\mathcal{F} = \frac{\partial\,\mathbf{W}(n)}{\partial\,\mathbf{l}_k}\,, \quad (k, n = 1,\, \ldots,\, N) \tag{15}$$

Here we assume that the vector $\mathbf{i}$, which specifies the interfaces, is such that the computed traveltimes and horizontal slowness components for each trial model exactly match those in the data. The NMO ellipses are computed using the formalism developed by Grechka and Tsvankin (1999).

Figure 3 shows a typical result of SVD analysis of the NMO ellipses with respect to the parameters $\mathbf{l} = \{V_{P0,1},\, \epsilon_1,\, \delta_1,\, V_{P0,2},\, \epsilon_2,\, \delta_2\}$ in a two-layer model. While the last singular value is always equal to zero, the other five do not vanish if the azimuths of the interfaces are different (see the curves marked by squares, diamonds and triangles). The presence of two vanishing singular values when the strikes of both interfaces coincide (the circles in Figure 3) is not surprising, because in this case the axes of the NMO ellipse from the bottom of the model are aligned with the dip and strike directions (i.e., the model becomes 2-D), and there is one less independent data component.

The model from Figure 3 can be used to support the statement that the inversion results are independent of the CMP location. We repeated our computation for a number of different common midpoints and obtained the same curves of singular values as those in Figure 3. Moreover, the singular values do not change when NMO ellipses computed at a number of CMP locations are used in the Frechét matrix (15) *simultaneously*. Therefore, it is indeed sufficient to carry out the inversion using the

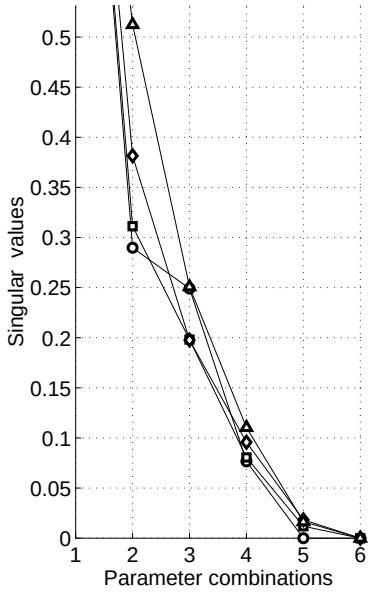

Figure 3. SVD analysis for a two-layer VTI model with the parameters $V_{P0,1} = 2$ km/s, $\epsilon_1 = 0.15$, $\delta_1 = 0.05$, $V_{P0,2} = 3$ km/s, $\epsilon_2 = 0.25$, $\delta_2 = 0.10$. The singular values are normalized by the greatest one. The interface depths under the CMP location $\mathbf{O} = [0, 0, 0]$ are $z_1 = 1$ km and $z_2 = 3$ km, the dips $\phi_1 = 40°$ and $\phi_2 = 20°$, and the azimuth of the bottom interface is $\psi_2 = 0°$. The curves correspond to different azimuths of the intermediate (first) interface: ○ ($\psi_1 = 0°$), □ ($\psi_1 = 30°$), ◇ ($\psi_1 = 60°$) and △ ($\psi_1 = 90°$).

NMO ellipses from all interfaces measured at a single CMP.

To get a more quantitative assessment of the feasibility of the inversion for the model from Figure 3, we performed a series of SVD analyses of the matrix W_{ij} for different values of the dip (ϕ_1) and azimuth (ψ_1) of the first interface. The results, displayed in Figure 4, indicate that it should be possible to estimate five parameter combinations for any ϕ_1 and ψ_1, except for $\psi_1 = 0°$, 180° and $\phi_1 = 0°$. In the first two cases, the two reflectors are co-oriented, and the 3-D model becomes 2-D, which reduces the number of equations to four. In the third case ($\phi_1 = 0°$), the first layer is horizontal and the NMO ellipse $W(1)$ degenerates into a circle that constrains just one combination of the medium parameters.

The observations drawn from Figures 3 and 4 can be extended to an arbitrary number of VTI layers. At a maximum, the NMO ellipses constrain $3N - 1$ combinations of the $3N$ interval parameters $\{V_{P0,n}, \epsilon_n, \delta_n\}$ ($n = 1, \ldots, N$), provided the model interfaces have different azimuths. Otherwise, P-wave traveltimes contain less information about the medium. For instance, if the azimuths of all interfaces are identical, the model degenerates into 2-D, and the NMO ellipses from different

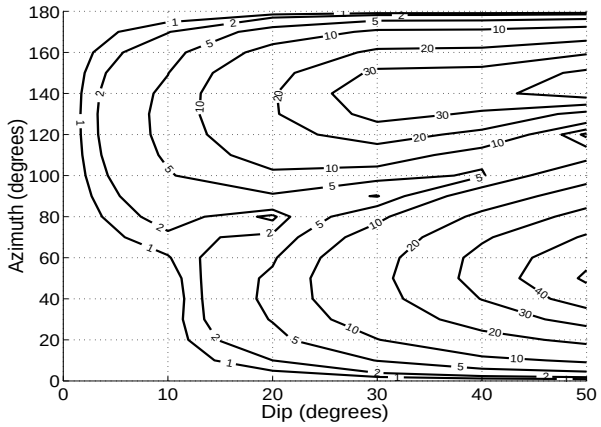

Figure 4. Contours of the fifth eigenvalue (multiplied by 1000) as a function of the dip ϕ_1 and azimuth ψ_1 of the intermediate interface in a two-layer VTI model. The parameters $V_{P0,1}$, ϵ_1, δ_1, $V_{P0,2}$, ϵ_2, δ_2, z_1, z_2, ϕ_2, and ψ_2 are the same as those in Figure 3.

reflectors are co-oriented. Thus, only their semi-axes constrain the layer parameters, and the number of independent equations reduces to $2N$. In the limiting case of horizontal layers, the NMO ellipses become circles defined by the N interval zero-dip NMO velocities [equation (1)]. Hence, unambiguous inversion is impossible without additional information; some practical possibilities are discussed below.

Parameter estimation using *a priori* information

Specifying one of the parameters

The results of the previous section suggest that *a priori* knowledge of a single layer parameter may be sufficient to overcome the ambiguity. For example, it might be possible to estimate the vertical velocity $V_{P0,1}$ in the top layer using a shallow borehole and then obtain the anisotropic parameters ϵ_1 and δ_1 from the NMO ellipse $\mathbf{W}(1)$. According to our SVD results, this should be sufficient for estimating the remaining medium parameters.

To verify this conclusion, we performed several numerical tests, with typical results listed in Table 1. We traced reflected rays through a three-layer VTI model for nine CMP locations (Figure 5 and Table 1), added Gaussian noise to the computed NMO velocities and zero-offset traveltimes, and found the layer parameters by least-squares fitting of the NMO ellipses. Although, as discussed above, multiple common midpoints do not provide new information for the inversion, they help to obtain more stable results in the presence of random noise.

To constrain the inversion, the parameter $\delta_1 = 0.04$ was assumed to be known, which allowed the other pa-

	$V_{P0,1}$ (km/s)	ϵ_1	δ_1	$V_{P0,2}$ (km/s)	ϵ_2	δ_2	$V_{P0,3}$ (km/s)	ϵ_3	δ_3
Correct	1.00	0.08	0.04	2.00	0.20	0.10	3.00	0.10	0.05
Inverted	0.99	0.09	–	2.02	0.18	0.09	2.96	0.18	0.07

	z_1 (km)	ϕ_1 (deg)	ψ_1 (deg)	z_2 (km)	ϕ_2 (deg)	ψ_2 (deg)	z_3 (km)	ϕ_3 (deg)	ψ_3 (deg)
Correct	1.00	30.0	–10.0	2.00	30.0	30.0	4.00	10.0	70.0
Inverted	1.00	29.8	–10.0	1.98	29.9	30.4	3.98	10.3	70.5

Table 1. Comparison of the correct and inverted parameters of a three-layer VTI model (see Figure 5). The standard deviation of Gaussian noise added to the NMO velocities and zero-offset traveltimes is 2.0% and 0.5%, respectively.

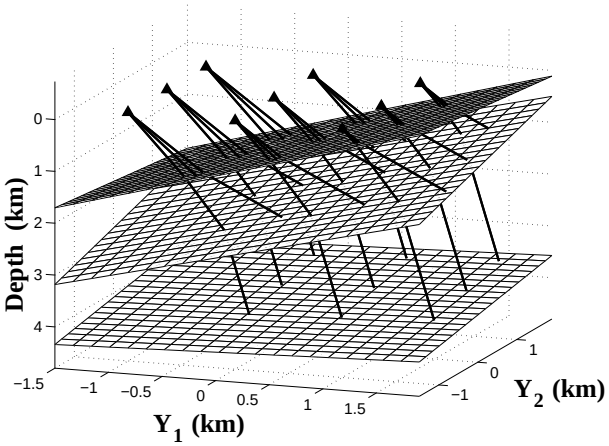

Figure 5. Zero-offset P-wave rays in the three-layer VTI model from Table 1.

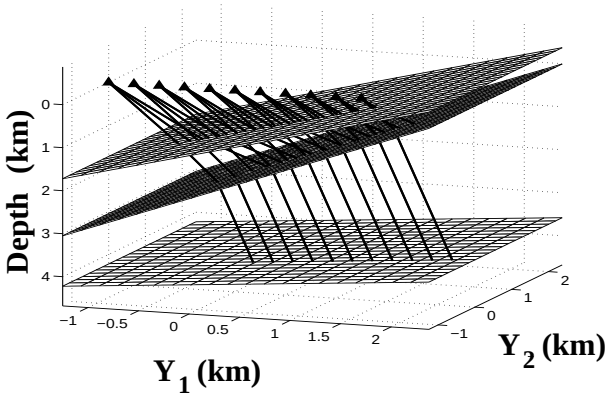

Figure 6. Zero-offset rays in a three-layer VTI model. All interfaces have the same azimuth $\psi_1 = \psi_2 = \psi_3 = 0°$.

rameters to be estimated with good accuracy (Table 1). The errors generally increase with depth, which can be expected from Dix-type algorithms. The low accuracy in the parameter ϵ_3 in the bottom layer is also associated with insufficient angle coverage of the reflected rays.

The choice of δ_1 as the known parameter was arbitrary; holding any other interval parameter at the correct value produces similar results. It is always possible to reconstruct the whole model if the vertical velocity $V_{P0,n}$ or one of the anisotropic coefficients (ϵ_n or δ_n) in any layer is known. The inversion procedure also works well in the special case of isotropy, i.e., when ϵ_n and δ_n are set to zero in one or more layers.

Specifying vertical velocity in 2-D models

We also examined the case when all interfaces in the three-layer medium discussed above have the same azimuth. The axes of the NMO ellipses W(1), W(2), and W(3) in such a model are parallel to the dip and strike directions, and the moveout data provide only six equations (two semi-axes for each ellipse). Since there is a total of nine medium parameters (three per layer), three parameters have to be specified in advance. One possibility, examined in the test from Figure 6 and Table 2, is to assume that the vertical velocities in the model are known, for example, from VSP data. We modeled zero-offset traveltimes and NMO ellipses for several CMP locations distributed along the dip direction (Figure 6) and performed the inversion of noise-contaminated data. The vertical velocities in each layer $V_{P0,1} = 1$ km/s, $V_{P0,2} = 2$ km/s, and $V_{P0,3} = 3$ km/s were assumed to be known. The inverted interval parameters ϵ_n and δ_n are in close agreement with the actual values (Table 2). Comparable accuracy was achieved in a number of other tests where we varied the number of layers and the level of noise.

Specifying a relationship between ϵ and δ

Another way to reduce the number of unknowns is to impose an empirical relationship between ϵ and δ, such as those discussed by Ryan-Grigor (1998), in at least one

	$V_{P0,1}$ (km/s)	ϵ_1	δ_1	$V_{P0,2}$ (km/s)	ϵ_2	δ_2	$V_{P0,3}$ (km/s)	ϵ_3	δ_3
Correct	1.00	0.08	0.04	2.00	0.20	0.10	3.00	0.10	0.05
Inverted	–	0.08	0.04	–	0.19	0.10	–	0.08	0.05

Table 2. Comparison of the correct and inverted values of parameters for the three-layer VTI model shown in Figure 6. The standard deviation of the Gaussian noise added to the traveltimes and NMO velocities is 1.0% and 2.0%, respectively.

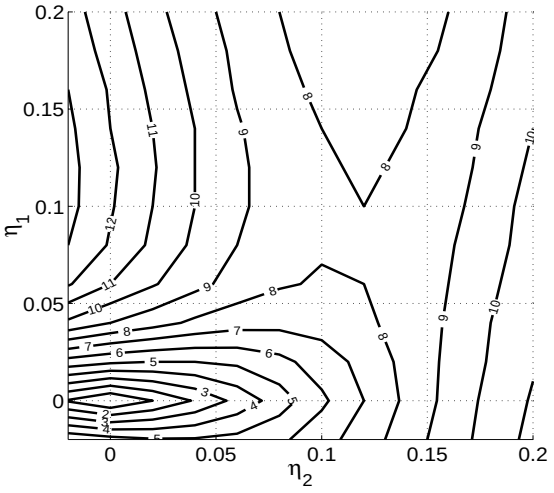

Figure 7. Contours of the smallest singular value (multiplied by 1000) for a two-layer VTI model. The relevant model parameters are $V_{P0,1} = 1$ km/s, $\epsilon_1 = 0.20$, $\delta_1 = k_1\,\epsilon_1$, $V_{P0,2} = 2$ km/s, $\epsilon_2 = 0.20$, $\delta_2 = k_2\,\epsilon_2$, $\phi_1 = 30°$, $\psi_1 = 30°$, $\phi_2 = 50°$, $\psi_2 = 0°$, $z_1 = 1$ km, $z_2 = 3$ km. The coefficients k_1 and k_2 vary from 0 to 1.1.

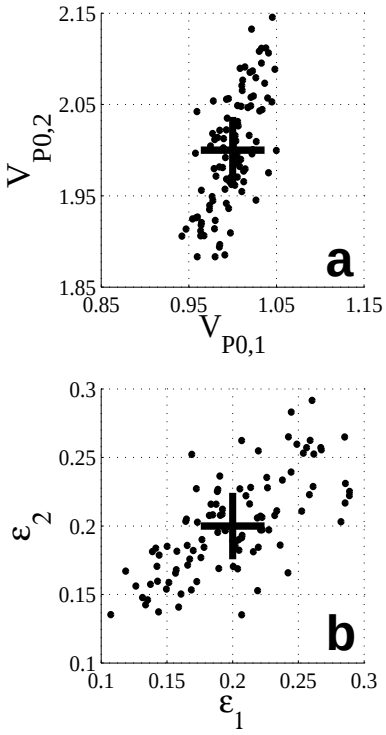

Figure 8. Comparison of the correct (crosses) and inverted (dots) values of parameters for the two-layer VTI model from Figure 7. k_1 and k_2 are such that $\eta_1 = \eta_2 = 0.05$. NMO velocities, computed at four CMP locations, were contaminated by Gaussian noise with a standard deviation of 2%.

layer. We found that making ϵ a known function of δ [i.e., $\epsilon = \epsilon(\delta)$] leads to unique parameter estimation unless the dependence $\epsilon(\delta)$ is already constrained by the reflection data. Let us assume, for example, that the relation between the interval ϵ_n and δ_n is linear ($\delta_n = k_n\,\epsilon_n$), with the coefficients k_n known *a priori*. Figure 7 displays the contours of the smallest singular value for a two-layer VTI model in which $\delta_1 = k_1\,\epsilon_1$ and $\delta_2 = k_2\,\epsilon_2$ (in principle, specifying k_1 alone would be sufficient). Although this singular value was computed as a function of k_1 and k_2, the axes in Figure 7 are labeled in terms of the anellipticity coefficients $\eta_n \equiv (\epsilon_n - \delta_n)/(1 + 2\,\delta_n)$ (for weak anisotropy, $\eta_n \approx \epsilon_n - \delta_n$) to demonstrate that the only vanishing singular value corresponds to elliptical anisotropy of the *whole* model ($\eta_1 = \eta_2 = 0$). If either $\eta_1 \neq 0$ or $\eta_2 \neq 0$, none of the eigenvalues goes to zero, and the inversion becomes feasible.

This is illustrated by the satisfactory inversion results for the model with $\eta_1 = \eta_2 = 0.05$ in Figure 8. We repeated the inversion 100 times for different realizations of Gaussian noise that was added to the NMO velocities. As Figure 8 shows, the standard deviations in the reconstructed anisotropic coefficients ϵ_1 and ϵ_2 are 0.036 and 0.044, respectively, while the values of vertical velocities $V_{P0,1}$ and $V_{P0,2}$ were recovered with standard deviations 2.5% and 3.2%.

One special case when this approach does *not* help is elliptical anisotropy. Even if all layers are known to be elliptically anisotropic ($k_n = 1$, $\epsilon_n = \delta_n$), and the number of the relevant VTI parameters reduces to $2N$, the $3N - 1$ equations for the NMO ellipses do not have a unique solution. This conclusion is in agreement with the results of Dellinger and Muir (1988) obtained using linear transformations (stretching) of the isotropic wave equation.

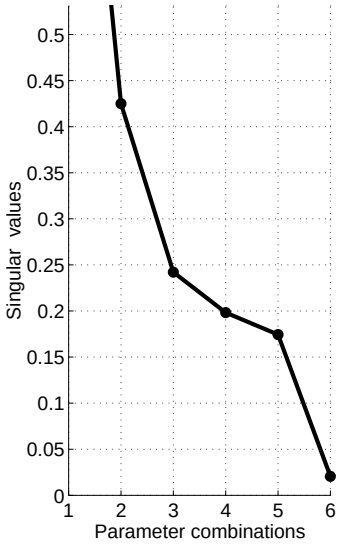

Figure 9. SVD analysis for a two-layer VTI model similar to the one in Figure 3. This time, however, the intermediate interface contains two segments with the same dip $\phi_1 = 40°$ but different azimuths $\psi_1 = 30°$ and $\psi_1 = 90°$.

Models with curved interfaces or faults

A priori information may not be needed at all for models with more than one plane reflector in some of the layers. The presence of different reflector dips causes reflected rays to span more spatial directions, which helps to constrain the anisotropic velocity model. While media with irregular interfaces are discussed in detail in a sequel paper, here we show how additional dips can remove the nonuniqueness in the parameter estimation.

Let us suppose, for example, that the intermediate interface in the two-layer VTI model from Figure 3 is bent in such a way that it has two plane portions with the same dip $\phi_1 = 40°$ but different azimuths $\psi_1 = 30°$ and $\psi_1 = 90°$. Recording reflections from the bottom of the model which cross both portions of the intermediate interface yields an additional NMO ellipse (i.e., three more equations). The absence of vanishing singular values for this problem (Figure 9; the smallest singular value is 0.02) indicates that all parameters can be resolved uniquely. We should note, however, that here we continue using the assumption that all layers are homogeneous.

Parameter estimation may also become feasible if the model contains a dipping fault plane, and the data include the reflections from both the fault and layer boundaries. A similar model was used by Alkhalifah and Tsvankin (1995), who developed a dip-moveout inversion method to estimate the interval values of η from surface P-wave data. Alkhalifah and Tsvankin (1995), however, assumed that each zero-offset reflected ray crosses only *horizontal* interfaces on its way to the surface.

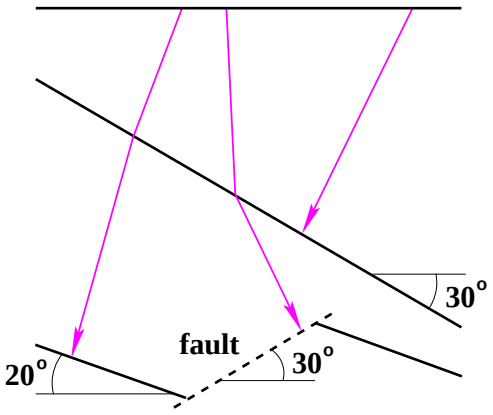

Figure 10. The presence of fault-plane reflections in layered VTI medium might be sufficient to obtain the model in depth using P-wave reflection data.

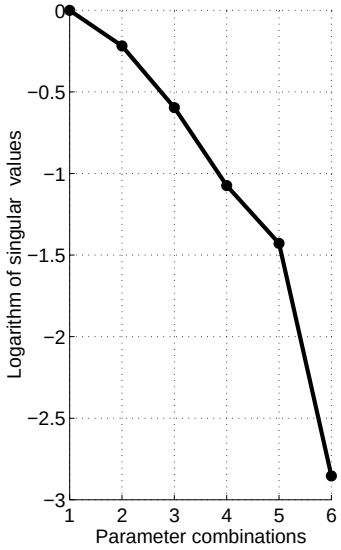

Figure 11. SVD analysis for the VTI model from Figure 10. The layer parameters are the same as those in Figure 3.

In our models (e.g., Figure 10), intermediate interfaces are dipping, which creates the dependence of NMO ellipses from both horizontal and dipping reflectors on the interval values of ϵ and δ. Even for 2-D media with fault planes in some of the layers, it may be possible to determine all relevant VTI parameters. For example, the semi-axes of the three NMO ellipses corresponding to the zero-offset rays marked in Figure 10 provide us with six equations. SVD analysis reveals no zero singular values which proves that the interval parameters can be found in a unique fashion (Figure 11). Still, the inverse problem is not as well-posed as that for 3-D models because

the smallest singular value in Figure 11 is just 0.0014 compared to 0.02 in Figure 9.

Discussion and conclusions

P-wave NMO ellipses measured from multi-azimuth 3-D reflection data over layered VTI media depend on all three relevant Thomsen parameters ($V_{0,n}$, ϵ_n and δ_n), if the overburden contains dipping interfaces. Here, we examined the inversion of P-wave traveltime data for the interval VTI parameters, the orientation (dip and azimuth) and depth of the interfaces. For each trial model the objective function, which has to be minimized during the inversion, is obtained in two steps. First, P-wave zero-offset traveltimes and reflection slopes (horizontal slownesses) are used to find the dip, azimuth and depth of all interfaces and reconstruct the trial model in depth. Second, we compute the effective NMO ellipses of reflection events and define the objective function as a measure of the difference between the modeled ellipses and those recovered from the data.

If the interfaces have different azimuths and do not cross each other, the P-wave NMO ellipses in an N-layer model yield $3N-1$ independent equations for the $3N$ interval VTI parameters $V_{0,n}$, ϵ_n and δ_n. Remarkably, the spatial variation of the NMO ellipses for this model does not provide any additional information for the inversion procedure. Therefore, in general surface 3-D P-wave data alone are insufficient to determine the unknown VTI parameters and reconstruct the interfaces in a unique fashion. For 2-D models with co-oriented interfaces, the axes of all NMO ellipses are parallel to the dip and strike directions, and the number of independent equations reduces to $2N$.

This ambiguity, however, can be overcome if a *single* parameter in any layer is known *a priori*. For example, in many cases the subsurface layer may be assumed to be isotropic ($\epsilon_1 = \delta_1 = 0$), or the vertical velocity in it may be estimated in a shallow borehole. The inversion can also be made unique by introducing a certain relationship between the parameters (e.g., between ϵ and δ) in at least one of the layers. The only model for which this approach fails to remove the ambiguity is elliptical anisotropy ($\epsilon_n = \delta_n$). For 2-D models it is necessary to specify one parameter for layer before the inversion; for instance, the vertical velocities may be known from VSP measurements.

The VTI parameters are generally better constrained by P-wave reflection data if the medium contains a fault plane or curved interfaces. We showed that for some types of models with intersecting interfaces the inversion does not require any *a priori* information. On the whole, our results indicate that for a range of laterally heterogeneous VTI models it is possible to build velocity models in depth (and, therefore, perform anisotropic depth imaging) using surface P-wave data.

Acknowledgments

We are grateful to members of A(nisotropy)-team of the Center for Wave Phenomena (CWP), Colorado School of Mines, for helpful discussions. We also thank Joe Dellinger (BP Amoco) for pointing out that elliptical anisotropy requires special consideration and Ken Larner (CSM) for his review of the manuscript. The support for this work was provided by the members of the Consortium Project on Seismic Inverse Methods for Complex Structures at CWP and by the United States Department of Energy (Award #DE-FG03-98ER14908).

References

Alkhalifah, T., Biondi, B., and Fomel, S., 1998, Time-domain processing in arbitrary inhomogeneous media: 68th Ann. Internat. Mtg., Soc. Expl. Geophys., Expanded Abstracts, 1756–1759.

Alkhalifah, T., and Tsvankin, I., 1995, Velocity analysis in transversely isotropic media: Geophysics, **60**, 1550–1566.

Bartel, D.C., Abriel, W.L., Meadows, M.A, and Hill, N.R., 1998, Determination of transversely isotropic velocity parameters at the Pluto Discovery, Gulf of Mexico: 68th Ann. Internat. Mtg., Soc. Expl. Geophys., Expanded Abstracts, 1269–1272.

Bube, K.P., and Meadows, M.A., 1997, On the null space in linearized anisotropic surface reflection tomography: 67th Ann. Internat. Mtg., Soc. Expl. Geophys., Expanded Abstracts, 1677–1680.

Dellinger, J., and Muir, F., 1988, Imaging reflections in elliptically anisotropic media: Geophysics, **53**, 1616–1618.

Grechka, V., and Tsvankin, I., 1998, 3-D description of normal moveout in anisotropic inhomogeneous media: Geophysics, **63**, 1079-1092.

Grechka, V., and Tsvankin, I., 1999a, 3-D moveout inversion in azimuthally anisotropic media with lateral velocity variation: Theory and a case study: Geophysics, **64**, 1202–1218.

Grechka, V., and Tsvankin, I., 1999b, NMO surfaces and Dix-type formulae in heterogeneous anisotropic media: 69th Ann. Internat. Mtg., Soc. Expl. Geophys., Expanded Abstracts, 1612–1615.

Grechka, V., Tsvankin, I., and Cohen, J.K., 1999, Generalized Dix equation and analytic treatment of normal-moveout velocity for anisotropic media: Geophys. Prosp., **47**, 117–148.

Le Stunff, Y., Grechka, V., and Tsvankin, I., 1999, Depth-domain velocity analysis in VTI media using surface P-wave data: Is it feasible? 69th Ann. Inter-

nat. Mtg., Soc. Expl. Geophys., Expanded Abstracts, 1604–1607.

Le Stunff, Y., Grenié, D., 1998, Taking into account a priori information in 3D tomography: 68th Ann. Internat. Mtg., Soc. Expl. Geophys., Expanded Abstracts, 1875–1878.

Le Stunff, Y., Jeannot, J.P., 1998, Pre-stack anisotropic depth imaging: 60th EAGE Conference, Extended Abstracts.

Ryan-Grigor, S., 1998, Empirical relationships between anellipticity and V_P/V_S in shales: Potential applications to AVO studies and anisotropic seismic processing: 68th Ann. Internat. Mtg., Soc. Expl. Geophys., Expanded Abstracts, 208–211.

Sexton, P., and Williamson, P., 1998, 3D anisotropic velocity estimation by model-based inversion of pre-stack traveltimes: 68th Ann. Internat. Mtg., Soc. Expl. Geophys., Expanded Abstracts, 1855–1858.

Thomsen, L., 1986, Weak elastic anisotropy: Geophysics, **51**, 1954–1966.

Tsvankin, I., 1996, P-wave signatures and notation for transversely isotropic media: An overview: Geophysics, **61**, 467–483.